

Figure 1. Absorption spectra of DNMAC in aqueous solution and in the presence and absence of PAMPS.

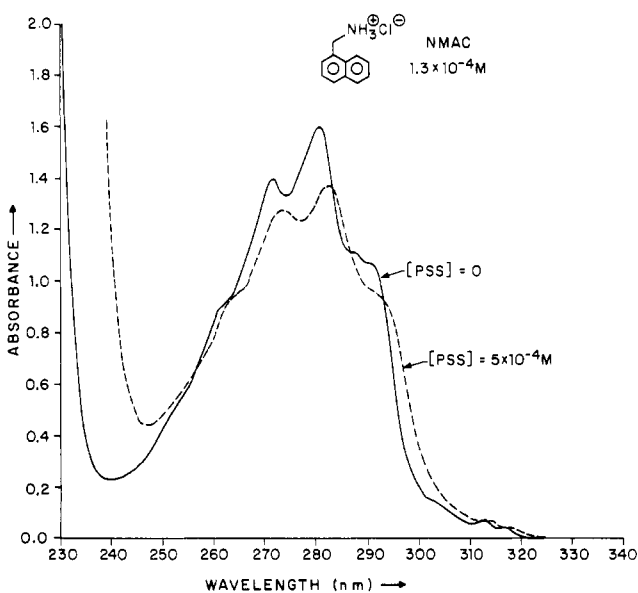


Figure 2. Absorption spectra of NMAC in aqueous solution and in the presence of PSS.

aromatic rings in the *ground state* of the probe. The ultraviolet spectrum of DNMAC and NMAC in water solution is composed of three major bands at 220, 280, and 315 nm, respectively. The latter two bands are shown in Figures 1–3. Analogous to naphthalene, the bands at 220 and 315 nm correspond to transitions along the long axis, and the band at 280 nm corresponds to transition along the short axis.<sup>3a</sup> Environmental polarity causes the vibrational resolution and the shifts in the maximum absorption wavelength of naphthalene to be modified.<sup>3a</sup> Association of naphthalene chromophores is known to influence these characteristics in a manner similar to those found to occur when DNMAC associates with a polyelectrolyte;<sup>6</sup> also, association of the probe with polyelectrolyte or change in pH of an aqueous solution of the probe causes analogous changes in the absorption spectrum of the probes (Figures 1–3).

The partial loss of vibrational fine structure of DNMAC (Figure 1) compared with NMAC (Figure 2) in pure water and the general red shift of the absorption band can both be ascribed to a small percent of dichromophoric molecules

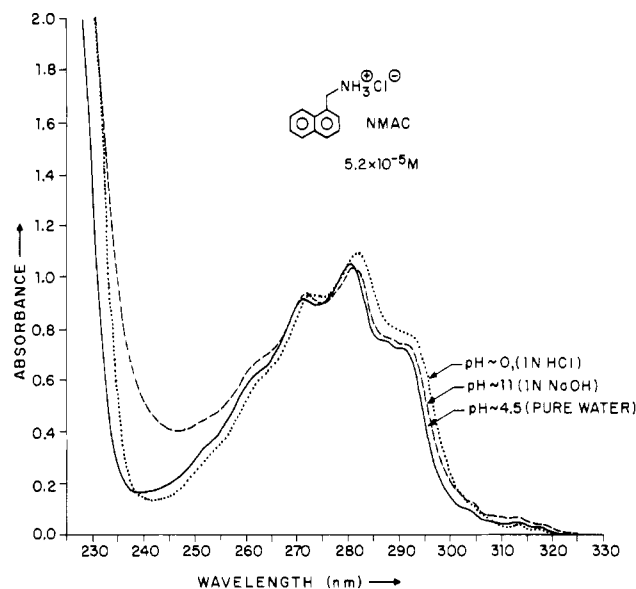


Figure 3. Absorption spectra of NMAC in aqueous solution at different pH.

that adopt the *gauche (+)*–*gauche (-)* conformation stabilized by the hydrophobic interaction of the two rings. The extent of stabilization of the *gauche (+)*–*gauche (-)* conformation when DNMAC interacts with the polyelectrolyte is confirmed by absorption spectra of the DNMAC–PAMPS system (Figure 1), for which the vibrational resolution is almost completely lost, not only in the short-axis absorption (280-nm band) but also in the long-axis absorption (315-nm band). Furthermore, the red shift is larger and the half-width of the band at 280 nm approaches  $6000\text{ cm}^{-1}$  compared with  $4500\text{ cm}^{-1}$  of NMAC in pure water. Interestingly, the association of a probe with the polyelectrolyte appears to modify not only the intramolecular conformational equilibrium (DNMAC) but also the spatial distribution of the probe's monomer units, e.g., in the analogous NMAC–PSS complex, in which preexcimer intermolecular dimers appear to be stabilized (Figure 2).

These results might be attributed to the result of a simple increase in local concentration of probe molecules, which results from sequestering by the polyelectrolyte. However, precedent in the literature<sup>3c</sup> suggests that the effect of an increase in local concentration is to broaden an absorption band, but not to shift the absorption maxima significantly. The broadening results from environmental effects on the absorbing species that cause the probe to experience numerous slightly different environments as absorption occurs. This, in turn, results in a general broadening of the absorption band but not in a shifting of the absorption maxima.

### Influence of pH

In a manner analogous to association with a polyelectrolyte, variation in pH causes substantial changes in the absorption spectra of the probes (Figures 1 and 3). The influence of pH can be ascribed to (a) changes in water structure or (b) alteration of acid–base equilibria such as those depicted in Scheme I. Amphiphilic molecules such as the probes employed in this study are believed to be surrounded by a cagelike water structure that is “open” in the region of the hydrophilic portion of the molecule.<sup>7</sup> In the transition from the tetrahedral form (1 in Scheme I) to the pyramidal form (3 in Scheme I), the water cage is closed (experimentally, when this occurs, the probe precipitates). Intermediate structures such as ion pairs,

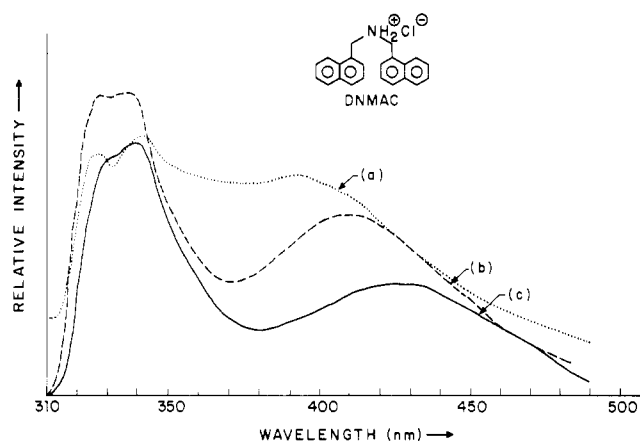


**Figure 4.** Emission spectra of DNMAC in aqueous solution at different pH: (a) pH  $\sim$ 5, pure water with a few drops of 1 N NaOH after filtration of the precipitate; (b) pH  $\sim$ 4.5, in pure water; (c) pH  $\sim$ 0, 1 N HCl. The excitation wavelength is 288 nm.

**Scheme I**

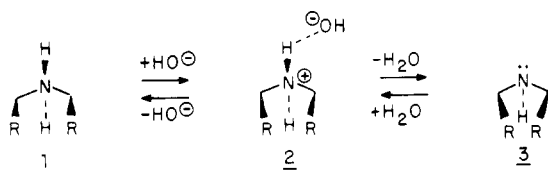


**Table I**

**pH Dependence of the Maximum Wavelength of the Monomer and Excimer Emission ( $\lambda_M^{\max}$ ,  $\lambda_E^{\max}$ ), the Excimer Exothermicity ( $\Delta\nu = 1/\lambda_M - 1/\lambda_E$ ), the Excimer to Monomer Intensity Ratio ( $I_E/I_M$ ), and the Excimer Lifetime  $\tau_E$  of DNMAC  $1 \times 10^{-4}$  M in Aqueous Solution**

pH	$\lambda_M^{\max}$ , nm	$\lambda_E^{\max}$ , nm	$\Delta\nu$ , $\text{cm}^{-1}$	$I_E/I_M$	$\tau_E$ , ns
0	338	420	5780	0.43	5
1	337	410	5280	0.50	11-16
4.5	335	405	5160	0.59	14-19
5 <sup>a</sup>	330	390	3770	0.84	6-16
11 <sup>a</sup>	330	385	3610	0.90	4-17

<sup>a</sup> After filtration of the precipitate.

2, may intervene as transients. The existence of such species is consistent with the observation of the variation of the emission spectra of DNMAC at different pHs (Figure 4). We postulate that as the pH increases, the tendency for the DNMAC to achieve the pyramidal structure produces changes in the geometry of the gauche (+)-gauche (-) conformation in such a way that the planes of the aromatic rings form a small angle and cannot be strictly parallel. A perfectly parallel disposition of the aromatic rings is not required for excimer formation and does not influence the excimer emission intensity.<sup>13</sup> However, the disposition of the aromatic rings is expected to affect the efficiency of the overlap that is required to stabilize the excimer complex. The excimer stability is measured<sup>2</sup> by  $\Delta\nu$  (Table I). At very low pH, structure 1 is the exclusive form and, according to Table I, can be characterized by a highly stabilized excimer complex ( $\Delta\nu = 5780 \text{ cm}^{-1}$ ). The smaller the overlap of the rings becomes, the smaller is the observed maximum wavelength of the excimer emission and the more pyramidal is the structure of the DNMAC. Simultaneously, the water cage becomes more closed and the eclipsed conformation is stabilized by the hydrophobic interaction of the two rings. In the absence of hydrophobic effects, the interaction between the aromatic rings is generally repulsive in the

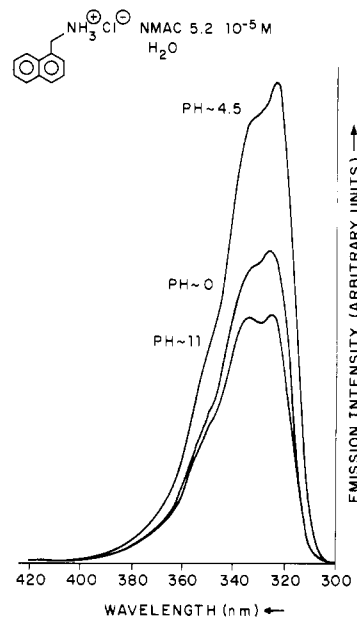


**Figure 5.** Emission spectra of NMAC in aqueous solution at different pH. The excitation wavelength is 288 nm.

ground state, but the eclipsed conformation minimizes the surface exposed to the water cage. This interpretation is consistent with the decrease of excimer emission at the lowest pH (Table I). The resulting modification of the water structure also causes changes in the vibrational resolution of the monomer emission (Figure 5) and monomer absorption (Figure 3). The unprotonated form 3 that is water insoluble is not expected to fluoresce, in analogy to other amines.<sup>5</sup> At sufficiently high pH, the unprotonated form precipitates from the aqueous phase.

### Fluorescence Decay

The kinetic analysis of the fluorescence of a dichromophoric molecule reveals the monomer emission shows a complex decay that is resolvable into a double exponential; however, the excimer emission shows only a single-exponential decay.<sup>14</sup> Such behavior is commonly, but not always, observed.<sup>8</sup> In some polymer systems, complex decays may be observed because of structural heterogeneities which exist on the time scale of emission. In small molecules, the coexistence of two or more different states of the chromophore or of two or more interactions (e.g., as is the case in systems involving proton transfer) may also cause complex decays.

The observed decay of the excimer emission (Figures 6 and 7) of DNMAC and NMAC shows only two first-order components in all the aqueous systems considered: (a) in pure aqueous solution, (b) with added *p*-toluenesulfonate (pTS), (c) with PSS, (d) with PAMPS, and (e) with poly(ethylene oxide) (PEO) in aqueous solution. Two excimer emissions are postulated for the DNMAC system: intermolecular and intramolecular excimer.<sup>1a</sup> Of course, only intermolecular excimer formation is possible in the case NMAC.

When the pH of the solution is changed, the slope of the two decays observed for the emission of DNMAC change. We interpret the decay behavior to result from different structures of the molecules in the ground state, i.e., forms 1 and 2 of Scheme I. At pH 0, only the protonated form 1 is present so that a single decay is observed, but at higher pH two emitting forms (1 and 2) exist, and a double decay is observed.

In methanol solution DNMAC has also a single decay that corresponds to a lifetime that is intermediate to that

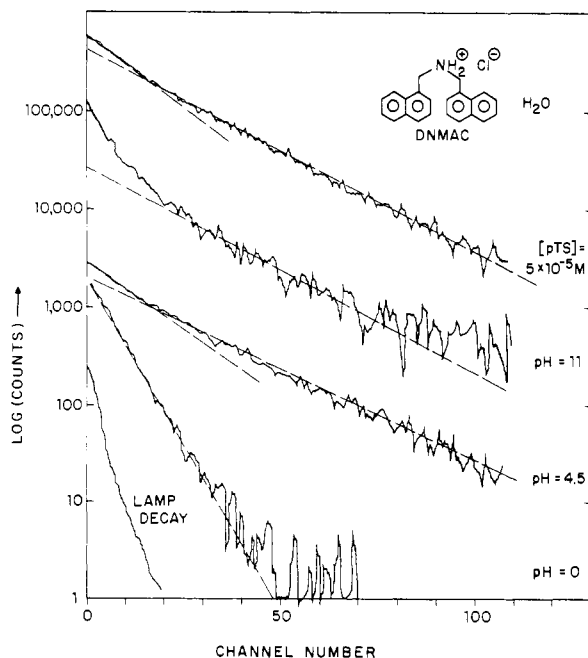


**Figure 6.** Fluorescence decay at 420 nm (excimer emission) of DNMAC ( $1 \times 10^{-4}$  M) in aqueous solution with pTS and at different pHs. The time per channel is 0.814 ns in all cases.

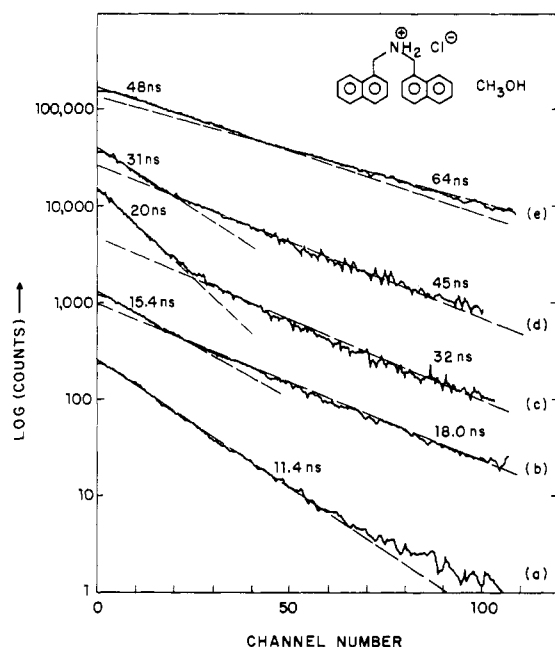


**Figure 7.** Excimer fluorescence decay at 400 nm of (a)  $7 \times 10^{-5}$  M DNMAC in methanol, (b) a mixture of  $7 \times 10^{-5}$  M DNMAC and  $7 \times 10^{-5}$  M PAMPS in methanol, (c) a mixture of  $7 \times 10^{-4}$  M DNMAC and  $0.4 \times 10^{-4}$  M PAMPS in water, (d) a mixture of  $1.0 \times 10^{-4}$  M DNMAC and  $3 \times 10^{-4}$  M PAMPS in water, and (e) a mixture of  $1.3 \times 10^{-4}$  M NMAC and  $4 \times 10^{-4}$  M PSS in water. For decays (a) and (b) the time per channel is 0.81 ns. For decays (c), (d), and (e) the time per channel is 1.62 ns. The excitation wavelength is 350 nm in all cases.

observed at high or at low pH. In methanol, only form 1 is expected to exist, but the dissociation of the chloride ion may be incomplete, given the smaller dielectric constant of the organic solvent compared to that of pure water. Upon association with PAMPS, the double decay is observed even in methanol. This result is consistent with the previous conclusion concerning the importance of electrostatic interactions in polyelectrolyte-probe interactions.<sup>1a</sup> If neutralization of the probe with a base has the same effect as the interaction of a probe and a po-

lyelectrolyte, then, in addition to atmospheric binding, there is probably a more localized and tighter binding of the polyelectrolyte-probe associate that causes a change in the structure of the probe into a form similar to 2.

Another consequence of formation of an associate is the increase of the lifetime of the monomer and of the excimer with respect to the probe in aqueous solution. This protection from quenching has also been observed when certain probes are complexed with cyclodextrins.<sup>4a</sup> It is unlikely to be due to a simple macroviscosity effect, since the addition of PEO does not significantly change the lifetime of DNMAC. However, the restrictions imposed on conformational mobility of DNMAC by the polyelectrolyte environment may be a significant factor in determining the long excimer lifetimes observed for the intramolecular excimer (Figure 7). The slopes of the two decays and their relative contribution to the overall intensity depend on the polyelectrolyte and probe concentrations in a manner analogous to that of the enhancement of the excimer emission (Figure 7). This result also supports the model discussed above involving partial neutralization of the probe.

## Conclusion

DNMAC and NMAC experience a strong interaction with polyelectrolytes via both hydrophobic and electrostatic forces. The accumulation of probes along the polymer chain favors the alignment of aromatic rings in a parallel conformation that avoids steric interactions, whereas the high local microviscosity of the probe environment inhibits conformational transition of the probes. The degree of binding depends on both the polymer and the probe concentrations. Binding produces a partial neutralization of the probe and the neutralized forms may exist for periods of up to 50 ns.

## Experimental Section

Polyelectrolytes were given to us by Prof. G. Gregor (Columbia University) and have been purified as previously described.<sup>1</sup> The synthesis and purification of the probes has also been previously described. Emission spectra were recorded on a Perkin-Elmer and a Hitachi spectrometer. Absorption spectra have been made on a Perkin-Elmer 559z UV/vis spectrophotometer. Fluorescence decay was measured by the single-photon-counting technique.<sup>9</sup>

**Acknowledgment.** We thank the National Science Foundation for generous support of this work. I.F.P. thanks the Fulbright Commission for a fellowship. We also thank Prof. H. Gregor (Columbia) and Dr. J. Emert (Exxon) for the samples of polyelectrolytes and probes, respectively.

**Registry No.** DNMAC, 17018-62-1; NMAC, 39110-74-2; PSS, 25704-18-1; PAMPS, 35641-59-9.

## References and Notes

- (1) (a) Turro, N. J.; Pierola, I. F. *J. Phys. Chem.*, in press. (b) Turro, N. J.; Okubo, T.; Emert, J.; Catena, R. *J. Am. Chem. Soc.* 1982, 104, 4799.
- (2) Frank, C. W. *Org. Coat. Plast. Chem.*, 1981, 45, 433.
- (3) (a) Riegelman, S.; Allawala, N. A.; Hrenoff, M. K.; Strait, L. A. *J. Colloid Sci.* 1958, 13, 208. (b) Strop, P.; Mikes, F.; Kalal, J. *J. Phys. Chem.* 1976, 80, 694.
- (4) (a) Turro, N. J.; Okubo, T.; Chung, C.-J. *J. Am. Chem. Soc.* 1982, 104, 1789. (b) Okubo, T.; Turro, N. J. *J. Phys. Chem.* 1981, 85, 4032.
- (5) (a) Goldenberg, M.; Emert, J.; Morawetz, H. *J. Am. Chem. Soc.* 1978, 100, 7171. (b) Emert, J.; Behrens, C.; Goldenberg, M. *Ibid.* 1979, 101, 771.
- (6) Irie, M.; Kamijo, T.; Aikawa, J.; Takemura, T.; Hayashi, K.; Baba, H. *J. Phys. Chem.* 1977, 81, 1571.
- (7) Tanford, Ch. "The Hydrophobic Effect. Formation of Micelles and Biological Membranes"; Wiley: New York, 1980.
- (8) Brand, L.; Ross, T. A. B.; Laws, W. R. *Ann. N.Y. Acad. Sci.* 1981, 366, 197.

- (9) Turro, N. J.; Tanimoto, Y. *Photochem. Photobiol.* **1981**, *34*, 173.  
 (10) Morawetz, H. *Science (Washington, D.C.)* **1979**, *203*, 405.  
 (11) Ito, S.; Yamamoto, M.; Nishijima, Y. *Bull. Chem. Soc. Jpn.* **1982**, *55*, 363.  
 (12) Turro, N. J.; Okubo, T. *J. Am. Chem. Soc.* **1982**, *104*, 2985.  
 The microviscosities reported for sodium poly(styrene-sulfonate) (PSS) are lower by a factor of 10 due to a mathe-

- tical error in the calculation based on molecular anisotropy. Thus the values of 150-100 cP reported in Table IV should be corrected to 15-11 cP. This correction places the microviscosity of PSS close to that of ionic micelles.  
 (13) Wang, Y. C.; Morawetz, H. *Makromol. Chem., Suppl.* **1975**, *1*, 283.  
 (14) Ghiggino, K.; Wright, R.; Phillips, D. J. *Polym. Sci., Polym. Phys. Ed.* **1978**, *16*, 1499.

## Representative Configurations of Unperturbed Poly(L-alanine) Chains

Dorothy Erie, J. A. Darsey, and Wayne L. Mattice\*

Department of Chemistry, Louisiana State University, Baton Rouge, Louisiana 70803.  
 Received September 15, 1982

**ABSTRACT:** Representative unperturbed poly(L-alanine) chains have been generated using Monte Carlo methods and the conformational energy surface obtained by Brant, Miller, and Flory (Brant, D. A.; Miller, W. G.; Flory, P. J. *J. Mol. Biol.* **1967**, *23*, 47-65). This conformational energy surface has previously been shown to reproduce unperturbed dimensions of several homopolypeptides and denatured proteins. Representative poly(L-alanine) chains have the overall character of a random coil. They contain no evidence whatsoever of  $\alpha$ -helical character at the local level. Instead there are occasional stretches that resemble the conformation adopted in the pleated sheet. These stretches may extend over as many as ten residues. They are of a length comparable to strands in the pleated sheets found in globular proteins. Propagation of the minimum-energy configuration would result in a left-handed helix with three residues per turn. In the representative chains, however, sequences that approximate a left-handed helix with three residues per turn occur much less frequently and are considerably shorter than sequences containing about two residues per turn. This situation arises because most unperturbed L-alanyl residues adopt conformations that are distributed over a rather broad region of low conformational energy. At one corner of this low-energy region lie conformations that can propagate a left-handed helix with three residues per turn. A longer traverse through the broad region of low conformational energy is found for a contour line on which lie conformations that would propagate a helix with two residues per turn.

Characteristic ratios,  $C$ , for polypeptides are conveniently defined as  $\langle r^2 \rangle_0 / n_p l_p^2$ , where  $\langle r^2 \rangle_0$  denotes the mean square unperturbed end-to-end distance for a chain containing  $n_p$  virtual bonds of length  $l_p$ .<sup>1</sup> Virtual bonds, of length 380 pm, link consecutive C $\alpha$  atoms when standard peptide units are retained in the planar trans configuration. Due to the difficulty in finding  $\theta$  solvents for disordered homopolypeptides, experimental characteristic ratios are usually based on measurements of the mean square perturbed dimensions in a good solvent. An estimation of the expansion coefficient is used to obtain  $\langle r^2 \rangle_0$ .<sup>1-6</sup> Experimental results have ranged from values as low as 2-3 for several sequential copolypeptides rich in glycyl residues<sup>4</sup> to values as large as 23 for poly(L-proline) in organic solvents at low temperature.<sup>3</sup> A much narrower range is obtained if attention is restricted to experimental results obtained with homopolypeptides bearing a CH<sub>2</sub>R side chain in the L configuration, as is shown in Table I. Characteristic ratios obtained for five such homopolypeptides fall in the range 8.6-10.

Characteristic ratios collected in Table I are subject to rationalization using a conformational energy surface computed for an unperturbed amino acid residue in poly(L-alanine). By evaluation of nonbonded interactions, intrinsic torsional potentials, and the electrostatic interaction of neighboring peptide units, Brant et al.<sup>8</sup> obtained a conformational energy surface that leads to a theoretical estimate of 9.3 for the characteristic ratio. This theoretical characteristic ratio is clearly in harmony with experimental results summarized in Table I. The conformational energy surface used to obtain a characteristic ratio of 9.3 is re-

drawn in Figure 1. The NMR coupling constant between the NH and C $\alpha$ H protons of several homopolypeptides is well reproduced with this energy surface.<sup>9</sup> It also satisfactorily accounts for dipole moments of 14 small alanine peptides when combined with a conformational energy surface for the D-alanyl residue, obtained by reflection through the origin.<sup>10</sup>

When used in conjunction with additional conformational energy surfaces required for polypeptides containing glycyl<sup>8,11</sup> or L-prolyl<sup>11,12</sup> residues, the conformational energy surface obtained by Brant et al.<sup>8</sup> permits calculation of unperturbed dimensions for denatured proteins. The dominant conformational energy surface for the residues of typical proteins low in glycyl and L-prolyl content is the one depicted in Figure 1. Results obtained in this manner have been quite impressive.<sup>13-15</sup> For example, light-scattering measurements conducted on the denatured, cross-linked tropomyosin dimer in 5 M guanidine hydrochloride<sup>16</sup> yield an unperturbed root-mean-square radius of gyration of 8.33 nm, which is in excellent agreement with the calculated value of 8.75 nm.<sup>14</sup> Bovine myelin basic protein in water is calculated to have an unperturbed root-mean-square radius of gyration of 4.64 nm,<sup>15</sup> while small-angle X-ray scattering yields an unperturbed root-mean-square radius of gyration of 4.56 nm.<sup>17</sup>

Since the conformational energy surface obtained by Brant et al.<sup>8</sup> has been shown to successfully capture many conformational characteristics of unperturbed amino acid residues bearing CH<sub>2</sub>R side chains, it becomes of interest to examine representative chains generated with this surface. Representative chains are depicted and described